Target Field Mapping and Uncertainty Estimation

Chao Gu

University of Virginia

cg2ja@virginia.edu

Feb 4, 2015

The E08-027 (g2p) experiment uses a 2.5 Tesla (5.0 T in some configurations) magnetic field to polarize the ammonia target. The map of this magnetic field is used to trace the trajectory of the out-going electrons and reconstruct the kinematics of them. So the uncertainty of the field map becomes an important contribution to the final uncertainty of the kinematics. In g2p experiment, the target field is generated by a pair of super-conducting Helmholtz coils and the field map of these coils is calculated directly from the Biot-Savart law. To estimate the uncertainty of the calculation, a measurement of the target field is performed during the experiment. This technical note will summarize the method of the measurement and give an estimation of the uncertainty of the field map.

1 Experiment Setup

It is difficult to place a Hall probe inside the target chamber so the field is measured several different positions on the surface of the target chamber. As shown in Figure 1, an aluminum block is used to keep a single-axis Hall probe perpendicular to the surface of the target chamber. The sensitive direction of this probe is radial direction so it reads B_r in the cylindrical coordinate system with respect to the axis of the target chamber. There is another Hall probe fixed to the block, with the sensitive direction setting to the azimuth direction to read B_ϕ. To determine the position of the measured points, four pieces of grid paper are attached to the target chamber. The aluminum block is aligned to the grid during the measurement and the position of each measured point is recorded with the coordinates of the grid paper. This gives the relative coordinates of each

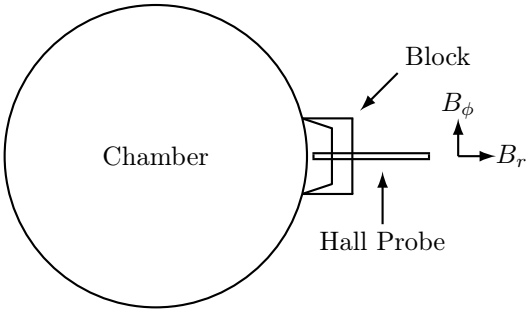

Figure 1: Sketch of the experiment setup. The azimuth direction Hall probe is not shown in this figure.

points with respect to the origin point of each grid paper. To determine the coordinates of the origin point of each grid paper in the Hall A coordinate system, three reference points on each paper are surveyed by the survey group. The position of each measured point can be obtained by adding some constant offset given by the geometry of the block and the structure of the probe to the readout coordinates of the grid paper. However, the target chamber may have a small deviation to the ideal vertical direction so the positions of the measured points need to be calibrated. Once the position of each point is determined, the theoretical B_r and B_ϕ can be interpolated from the field map and compare to the data. This also need to be calibrated first since the sensitive direction of the Hall probe may not align to the radial direction and azimuth direction perfectly.

2 Data Calibration

The survey result of the reference points on each graph paper is listed in Table 1. As mentioned in section 1, in reality the target chamber is not perfectly aligned to the origin point and the vertical direction. The offset (x_0, y_0, z_0) of the center of the target chamber and two azimuth angle (θ, ϕ) of the axis of the cylindrical chamber are five free parameters which need to be calibrated with the survey data. To accomplish this, the survey result of these reference points is used to fit the equation of the surface of the target chamber, which is a cylindrical surface. Although the radius (r) of the target chamber is known to be 469.6 mm, it is still considered as an additional free parameter in the fitting to give a cross-check.

The fitting result is shown in Table 2 and Figure 2. The positive z direction of the Hall A coordinate system is downstream along the beamline and positive x is to the beam right. The space and angle deviations of the target chamber are relatively small and the radius of the target chamber matches the design value

Paper	Point	grid x/cm	grid y/cm	x/mm	y/mm	z/mm
A	1	0.5	0.5	-242.9	413.5	-65.7
A	2	20.0	0.0	-389.3	280.5	-65.7
A	3	0.0	40.5	-242.5	414.2	338.7
B	1	0.5	0.5	-433.4	206.1	96.5
B	2	34.5	0.5	-463.7	-124.4	96.3
B	3	0.5	24.5	-433.5	206.1	336.7
C	1	0.5	0.5	-457.2	-146.5	96.6
C	2	40.0	0.5	-203.5	-434.6	95.9
C	3	0.5	24.5	-456.9	-147.1	336.6
D	1	0.5	0.5	-457.3	-146.1	-168.7
D	2	40.0	0.5	-204.7	-434.3	-171.1
D	3	0.5	24.5	-457.1	-146.6	71.2

Table 1: Survey result of the graph paper. x, y, z are in Hall A coordinate system. Grid x and Grid y is the coordinates of each point in the grid paper.

469.6 mm quite well.

By using the calibration result of the target chamber, the recorded coordinates of the data points can be converted to the coordinates in Hall A coordinate system. Firstly, the coordinates of the origin point of each grid paper is converted to the cylindrical coordinate of the target chamber. For each measured point, the

x_0/mm	y_0/mm	z_0/mm	θ/rad	ϕ/rad	r/mm
-0.21	0.00	-0.41	1.5709	1.5799	469.62

Table 2: Fitting result of the offset and orientation of the target chamber. x_0, y_0, z_0 are in Hall A coordinate system. θ, ϕ are azimuth angles with respect to the z axis of the Hall A coordinate system.

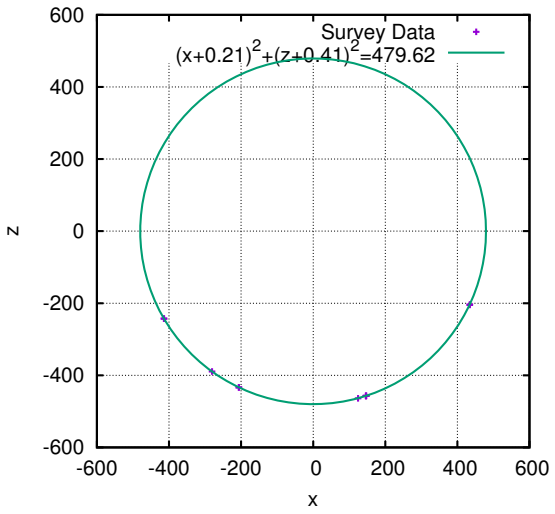

Figure 2: This figure shows that all survey points fits the same cylindrical surface after calibration.

recorded grid coordinates is actually the increments of the ϕ and z coordinates in the cylindrical coordinate of the target chamber. Once the coordinates of each data point is calculated in the cylindrical coordinate of the chamber, is is converted back to the Hall A coordinate system using the fitting results above. Table 3 shows the coordinates of each measured point after calibration.

ID	Paper	grid x/cm	grid y/cm	r/mm	ϕ/rad	h/mm	x/mm	y/mm	z/mm
1	A	0.0	35.0	479.62	0.5282	284.18	414.08	283.78	-242.54
2	A	5.0	35.0	479.62	0.6321	284.15	386.75	283.78	-284.15
3	A	10.0	35.0	479.62	0.7359	284.13	355.26	283.77	-322.71
4	A	15.0	35.0	479.62	0.8398	284.10	319.94	283.78	-357.79
5	A	20.0	35.0	479.62	0.9436	284.07	281.17	283.78	-389.02
6	A	25.0	35.0	479.62	1.0474	284.04	239.38	283.79	-416.07
7	A	0.0	25.0	479.62	0.5285	184.33	413.92	183.93	-242.65
8	A	5.0	25.0	479.62	0.6323	184.30	386.58	183.92	-284.25
9	A	10.0	25.0	479.62	0.7362	184.27	355.08	183.92	-322.80
10	A	15.0	25.0	479.62	0.8400	184.25	319.75	183.92	-357.87
11	A	0.0	15.0	479.62	0.5288	84.48	413.76	84.08	-242.75
12	A	5.0	15.0	479.62	0.6326	84.45	386.41	84.07	-284.35
13	A	10.0	15.0	479.62	0.7365	84.42	354.90	84.07	-322.89
14	A	0.0	5.0	479.62	0.5290	-15.37	413.60	-15.77	-242.86
15	A	5.0	5.0	479.62	0.6329	-15.40	386.24	-15.78	-284.45
16	A	10.0	5.0	479.62	0.7367	-15.43	354.72	-15.78	-322.98
17	B	0.0	13.0	479.62	1.1152	221.83	210.61	221.61	-431.32
18	B	5.0	13.0	479.62	1.2192	221.76	164.78	221.57	-450.84
19	B	10.0	13.0	479.62	1.3231	221.68	117.17	221.54	-465.51
20	B	15.0	13.0	479.62	1.4270	221.61	68.30	221.51	-475.15
21	B	20.0	13.0	479.62	1.5309	221.53	18.69	221.49	-479.67
22	B	25.0	13.0	479.62	1.6348	221.46	-31.12	221.46	-479.03
23	B	30.0	13.0	479.62	1.7387	221.38	-80.59	221.43	-473.22
24	B	0.0	20.0	479.62	1.1154	291.89	210.61	291.67	-431.36
25	B	5.0	20.0	479.62	1.2193	291.82	164.78	291.63	-450.87
26	B	10.0	20.0	479.62	1.3232	291.74	117.17	291.60	-465.53
27	B	15.0	20.0	479.62	1.4271	291.67	68.30	291.57	-475.17
28	B	20.0	20.0	479.62	1.5310	291.59	18.69	291.54	-479.68
29	B	25.0	20.0	479.62	1.6349	291.52	-31.12	291.52	-479.03
30	B	30.0	20.0	479.62	1.7388	291.44	-80.60	291.49	-473.21
31	C	0.0	20.0	479.62	1.8711	291.50	-142.22	291.61	-458.45
32	C	9.5	20.0	479.62	2.0691	291.27	-229.55	291.45	-421.51
33	C	20.0	20.0	479.62	2.2880	291.01	-315.51	291.28	-361.60
34	C	28.0	20.0	479.62	2.4547	290.81	-371.09	291.13	-304.21
35	C	0.0	13.0	479.62	1.8705	221.50	-142.04	221.61	-458.52
36	C	9.5	13.0	479.62	2.0686	221.27	-229.39	221.45	-421.63
37	C	20.0	13.0	479.62	2.2874	221.01	-315.38	221.28	-361.77

continued on next page

continued from previous page									
ID	Paper	grid x/cm	grid y/cm	r/mm	ϕ/rad	h/mm	x/mm	y/mm	z/mm
38	C	28.0	13.0	479.62	2.4542	220.81	-370.99	221.13	-304.40
39	C	0.0	5.0	479.62	1.8699	141.50	-141.83	141.61	-458.61
40	C	9.5	5.0	479.62	2.0679	141.27	-229.21	141.45	-421.76
41	C	20.0	5.0	479.62	2.2868	141.01	-315.23	141.28	-361.95
42	C	28.0	5.0	479.62	2.4536	140.81	-370.88	141.13	-304.62
43	D	0.0	24.0	479.62	1.8698	66.13	-141.84	66.23	-458.62
44	D	9.5	24.0	479.62	2.0675	65.48	-229.07	65.67	-421.87
45	D	20.0	24.0	479.62	2.2860	64.77	-314.99	65.04	-362.22
46	D	28.0	24.0	479.62	2.4524	64.22	-370.60	64.55	-305.04
47	D	0.0	16.0	479.62	1.8692	-13.84	-141.67	-13.74	-458.69
48	D	9.5	16.0	479.62	2.0669	-14.48	-228.93	-14.30	-421.98
49	D	20.0	16.0	479.62	2.2854	-15.20	-314.88	-14.93	-362.38
50	D	28.0	16.0	479.62	2.4519	-15.74	-370.51	-15.42	-305.23

Table 3: Coordinates of measured points. r, ϕ, h are cylindrical coordinate system with respect to the axis of the target chamber.

The theoretical field B_r, B_ϕ and B_h can be interpolated from the field map with the coordinates of each data point. If the Hall probes are perfectly aligned to their ideal direction, the readout of the probes should be directly comparable with the theoretical field result. However, there may be some small deviation of the sensitive direction of the probes. The mechanical errors when placing the Hall probe to the aluminum block also causes some offsets to the recorded position of the data points. Thus, the space offset (r_0, ϕ_0, h_0) with respect to the measured position and azimuth angle (θ, ϕ) with respect to the B_r direction are considered to be five free parameters of the probes (each probe has independent parameters). The measured field is used to do a fitting to determine these parameters. The fitting result is shown in Table 4.

Once the offset and the orientation of the two Hall probes are determined, the theoretical readout of these two probes could be calculated from the field map and compared with data. Table 5, Figure 3 and Figure 4 shows the measurement results. Figure 5 shows the differences between the measured fields and the field map. The average deviations between the measured fields and the field map are 4.66 gauss for B_r and 4.34 gauss for B_ϕ.

Probe	r_0/mm	ϕ_0/rad	h_0/mm	θ/rad	ϕ/rad
r	10.74	0.1351	0.00	0.0983	3.5197
ϕ	16.17	0.1351	-4.01	1.5032	3.1346

Table 4: Fitting result of the offset and orientation of the Hall probes. r_0, ϕ_0, h_0 are in the cylindrical coordinate system of the target chamber. θ and ϕ are azimuth angles with respect to the B_r direction.

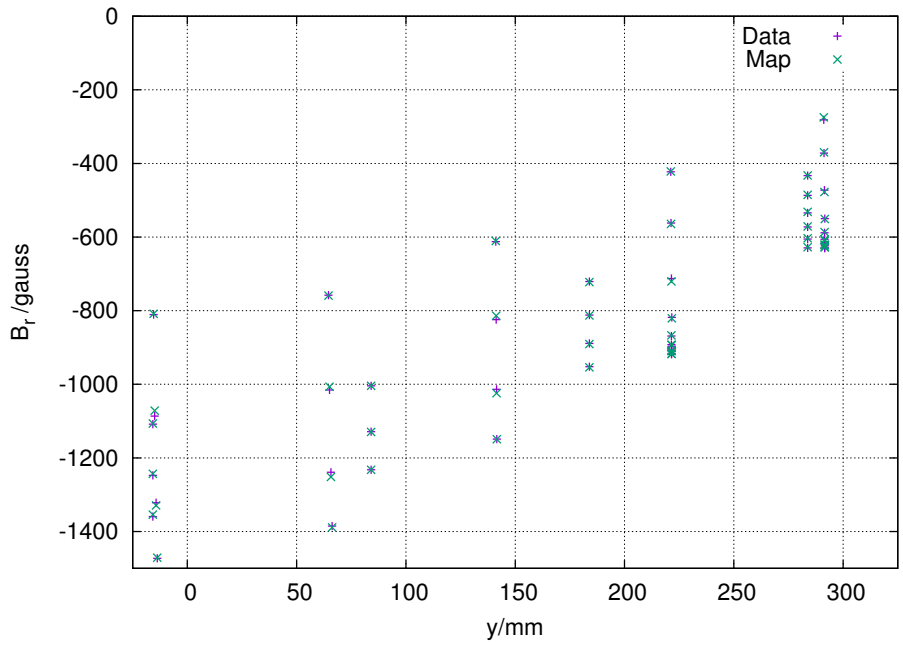

Figure 3: Measurement result of B_r (Data) and the calibrated value from the field map (Map).

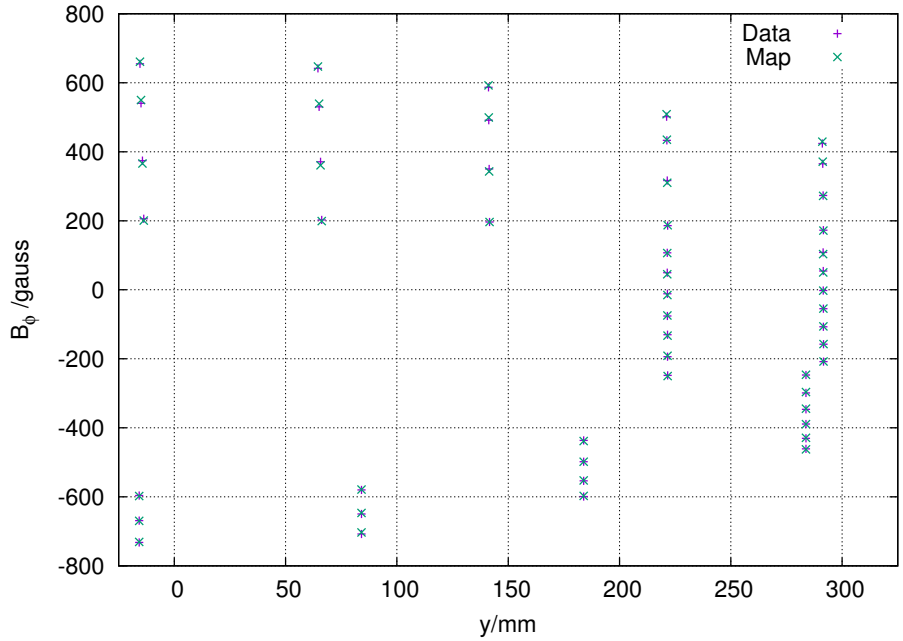

Figure 4: Measurement result of B_ϕ (Data) and the calibrated value from the field map (Map).

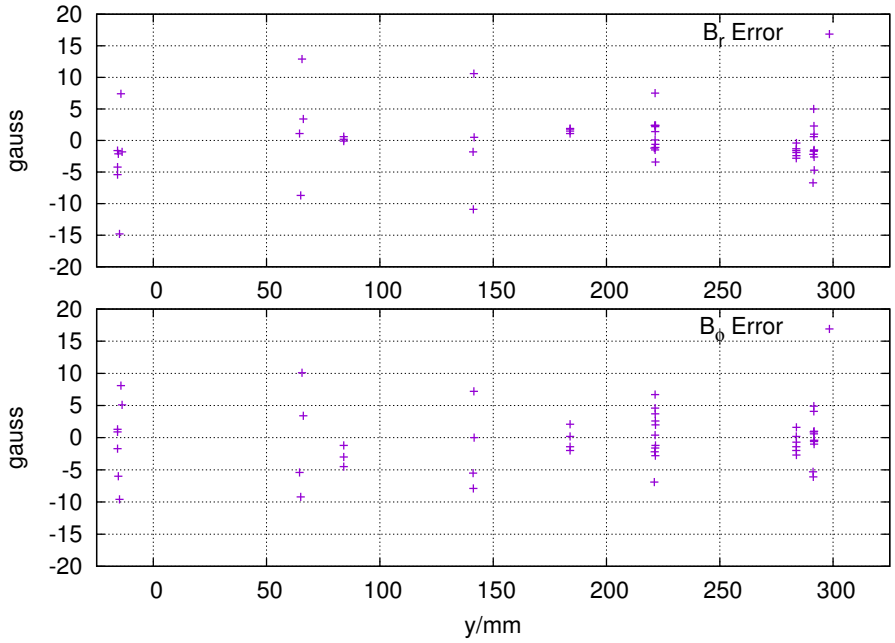

Figure 5: The distribution of the differences between the measured field and the field map.

ID	x/mm	y/mm	z/mm	B_r^{data}	B_r^{map}	B_r^{error}	B_ϕ^{data}	B_ϕ^{map}	B_ϕ^{error}
1	414.08	283.78	-242.54	-433.0	-432.6	-0.4	-460.8	-462.4	1.6
2	386.75	283.78	-284.15	-486.8	-485.2	-1.6	-430.5	-429.1	-1.4
3	355.26	283.77	-322.71	-534.5	-531.7	-2.8	-389.1	-389.3	0.2
4	319.94	283.78	-357.79	-572.4	-571.1	-1.3	-346.5	-344.5	-2.0
5	281.17	283.78	-389.02	-605.5	-603.1	-2.4	-299.1	-296.4	-2.7
6	239.38	283.79	-416.07	-629.4	-627.5	-1.9	-246.8	-246.1	-0.7
7	413.92	183.93	-242.65	-720.9	-722.4	1.5	-599.2	-597.2	-2.0
8	386.58	183.92	-284.25	-812.1	-813.2	1.1	-553.8	-552.4	-1.4
9	355.08	183.92	-322.80	-889.1	-890.9	1.8	-498.1	-498.3	0.2
10	319.75	183.92	-357.87	-952.2	-954.1	1.9	-436.3	-438.4	2.1
11	413.76	84.08	-242.75	-1004.0	-1004.2	0.2	-707.7	-703.2	-4.5
12	386.41	84.07	-284.35	-1128.8	-1129.4	0.6	-649.5	-646.5	-3.0
13	354.90	84.07	-322.89	-1232.3	-1232.2	-0.1	-579.9	-578.7	-1.2
14	413.60	-15.77	-242.86	-1108.2	-1106.6	-1.6	-732.2	-730.5	-1.7
15	386.24	-15.78	-284.45	-1247.6	-1243.4	-4.2	-668.9	-669.8	0.9
16	354.72	-15.78	-322.98	-1359.4	-1354.0	-5.4	-596.3	-597.6	1.3
17	210.61	221.61	-431.32	-896.8	-893.4	-3.4	-248.0	-250.0	2.0
18	164.78	221.57	-450.84	-910.4	-909.8	-0.6	-194.0	-191.2	-2.8
19	117.17	221.54	-465.51	-918.7	-917.6	-1.1	-130.2	-132.8	2.6
20	68.30	221.51	-475.15	-915.9	-917.3	1.4	-75.9	-74.3	-1.6
21	18.69	221.49	-479.67	-906.7	-908.9	2.2	-11.5	-15.2	3.7
22	-31.12	221.46	-479.03	-892.3	-892.4	0.1	49.5	44.9	4.6

continued on next page

continued from previous page									
ID	x/mm	y/mm	z/mm	B_r^{data}	B_r^{map}	B_r^{error}	B_ϕ^{data}	B_ϕ^{map}	B_ϕ^{error}
23	-80.59	221.43	-473.22	-868.7	-867.2	-1.5	107.0	106.6	0.4
24	210.61	291.67	-431.36	-614.8	-610.1	-4.7	-208.3	-207.9	-0.4
25	164.78	291.63	-450.87	-623.8	-622.3	-1.5	-157.8	-157.2	-0.6
26	117.17	291.60	-465.53	-630.5	-627.9	-2.6	-107.0	-106.0	-1.0
27	68.30	291.57	-475.17	-628.8	-627.2	-1.6	-55.0	-54.5	-0.5
28	18.69	291.54	-479.68	-617.8	-620.1	2.3	-1.9	-2.5	0.6
29	-31.12	291.52	-479.03	-606.1	-606.7	0.6	54.3	50.2	4.1
30	-80.60	291.49	-473.21	-588.4	-586.7	-1.7	108.3	103.4	4.9
31	-142.22	291.61	-458.45	-549.9	-550.9	1.0	172.7	171.7	1.0
32	-229.55	291.45	-421.51	-472.6	-477.6	5.0	273.2	272.3	0.9
33	-315.51	291.28	-361.60	-372.0	-369.8	-2.2	365.1	371.2	-6.1
34	-371.09	291.13	-304.21	-281.5	-274.8	-6.7	424.0	429.3	-5.3
35	-142.04	221.61	-458.52	-818.3	-820.7	2.4	185.9	187.1	-1.2
36	-229.39	221.45	-421.63	-712.9	-720.4	7.5	316.8	310.1	6.7
37	-315.38	221.28	-361.77	-562.0	-564.4	2.4	432.9	435.1	-2.2
38	-370.99	221.13	-304.40	-422.9	-421.7	-1.2	501.7	508.6	-6.9
39	-141.83	141.61	-458.61	-1148.9	-1149.4	0.5	196.3	196.3	0.0
40	-229.21	141.45	-421.76	-1013.6	-1024.2	10.6	350.3	343.1	7.2
41	-315.23	141.28	-361.95	-824.5	-813.6	-10.9	491.6	499.5	-7.9
42	-370.88	141.13	-304.62	-612.3	-610.5	-1.8	586.8	592.3	-5.5
43	-141.84	66.23	-458.62	-1385.2	-1388.6	3.4	202.5	199.1	3.4
44	-229.07	65.67	-421.87	-1238.9	-1251.8	12.9	371.0	360.9	10.1
45	-314.99	65.04	-362.22	-1015.3	-1006.6	-8.7	530.2	539.4	-9.2
46	-370.60	64.55	-305.04	-757.9	-759.0	1.1	641.6	647.0	-5.4
47	-141.67	-13.74	-458.69	-1472.7	-1470.9	-1.8	205.9	200.8	5.1
48	-228.93	-14.30	-421.98	-1321.8	-1329.2	7.4	374.2	366.1	8.1
49	-314.88	-14.93	-362.38	-1086.4	-1071.6	-14.8	540.3	549.9	-9.6
50	-370.51	-15.42	-305.23	-810.6	-808.5	-2.1	654.8	660.8	-6.0

Table 5: Compare between the field map and the measured field. The unit of fields is gauss.

3 Uncertainty Estimation

The average deviations between the measured fields and the field map have been calculated in section 2. The value is close to 5 gauss around the target chamber. However, this result has assumed that the calibration of the orientation of the Hall probes is accurate. Since it is difficult to be verified with real measurement, this assumption may not be true. The influence of the orientation of the Hall probes to the uncertainty of the measured field can be estimated by adding an uncertainty of certain level to the azimuth angle of the probes and recalculate the average deviations between the measured fields and the predicted values from the field map. Two situations is tested here to estimate the uncertainty. If the azimuth angle of the probes is

increased by 10 mrad, the average deviations increase to 6.71 gauss for B_r and 10.18 gauss for B_ϕ. If the azimuth angle of the probes is decreased by 10 mrad, the average deviations increase to 6.67 gauss for B_r and 10.17 gauss for B_ϕ. So it is safe for us to conclude that the uncertainty of this measurement is less than 12 gauss and the relative uncertainty is 1.2% (the average field strength around the target chamber is ∼1000 gauss).

The angle deviation of a charged particle in a static magnetic field can be expressed by equation:

$$\Delta\theta = \frac{q}{mv}\int_L B \cdot \mathrm{d}l \tag{1}$$

the integration is along the trajectory of the particle. Thus, the uncertainty of the target field need to be propagate to the integration of $B \cdot \mathrm{d}l$ to give its contribution of the uncertainty of the kinematics variables. The uncertainty of the target field outside the target field has been estimated above. During the experiment, the field strength at the target center is monitored by NMR method. The relative uncertainty of this method is less than 0.1%. The uncertainty of the target field in the other region of the target chamber is not known, so an interpolation between 0.1% and 1.2% will be used when applying equation 1. The simulation package is used to calculate the integrated $B \cdot \mathrm{d}l$. With a 2.5 T transverse target field, the integrated $B \cdot \mathrm{d}l$ is 6.682×10^{-1} T·m, and the uncertainty is 5.682×10^{-3} T·m, the relative uncertainty is 0.85%. Thus, the contribution of the uncertainty of the target field map to the scattering angle is about 0.85%.